Design And Simulation of Autonomous Parachute System For Unmanned Aerial Vehicle

Umang Srivastava[1], Dr. Anand Swaroop Verma[2]
[1, 2] Dept of MECHANICAL ENGINEERING
[1, 2] Kanpur Institute of Technology, Rooma, Kanpur

Abstract- *The project aims at Slybird which is a mini-unmanned aerial vehicle developed by National Aerospace laboratories. NAL Slybird is hand launched and with a soft landing recovery capability. It has an endurance of one hour with a range of 10 km. Its operational altitude is 300 meters and a service ceiling altitude of 15000 feet. The UAV has belly landing which creates a problem for it to land on any terrain. So as to solve the problems faced during landing we are here designing a recovery system for it so that it can be slowed down while landing and it also remains safe on any terrain.*
During belly landing, there is normally extensive damage to the UAV's. Belly landings carry the risk that the aircraft may flip over, disintegrate also it can catch fire if it lands too fast or too hard. Extra care should be taken while the UAV lands that is straight and level as possible also it should be having enough airspeed to maintain control over the UAV. The danger of performing belly landing increases with the involvement of strong crosswinds, damage to the airplane, or unresponsive instruments or controls. Thus here we are designing a suitable parachute for safe recovery of the UAV so as to reduce the kinetic energy of the UAV when it descends and performs landing.

The project comprises of the mathematical calculations as well as the designing procedure of the two as well as six degree-of-freedom models which extensively give details about the trajectory of the falling parachute with the UAV. The model generated using SIMULINK is capable of generating trajectory even in wind conditions and thus gives a real feel of how the real parachute would fall. The automated deployment system which is also presented here using Arduino microcontroller and other sensors is good enough to handle the deployment of the parachute at any type of problem if occurs during flight of UAV.

Thus the project aims at designing an automated parachute system for the Unmanned Aerial Vehicles.

List of Abbreviations

α	Angle of attack
$??_{??}$	Mach number
{??}	Body-fixed coordinate frame
$??_{??}$	Aerodynamic drag coefficient of undisturbed canopy
$??_{??}$	Aerodynamic moment coefficient of undisturbed canopy
$??_{??}$	Yaw moment cause by yaw acceleration
??	Vector of external force
$??^{????}$	Total aerodynamic force vector
$??_{????????}$	Aerodynamic force vector of undisturbed canopy
??	Gravitation vector caused by Earth's gravity g
$??_{??}$	Moment of inertia about axis of {b}
$??_{???}$	Length of suspension lines
??	Vector of external moment
$??_{????????}$	Aerodynamic moment vector of undisturbed canopy
$????^{??}_{??}$	Moments caused by the weight of the i^{th} component when being translated to the center of gravity of the whole system
$??^{????}$	Total aerodynamic moment vector
$??_{??}$	Mass of the i^{th} component
??	Dynamic pressure
$??_{??}$	Radius of inflated parachute
$??_{0}$	Reference radius of un inflated canopy
$??^{??}_{??}$	Rotation matrix from {b} to {u}
$??_{0}$	Canopy's reference area
{u}	Local tangent plane coordinate frame
$??_{??}$	Wind vector measured in {u}
$??_{???}$	Spatial angle of attack
ε	Canopy shape ratio

I. INTRODUCTION

The project aims at Slybird which is a mini-unmanned aerial vehicle developed by National Aerospace laboratories. NAL Slybird is hand launched and with a soft landing recovery capability. It has an endurance of one hour with a range of 10 km. Its operational altitude is 300 meters and a service ceiling altitude of 15000 feet.

During belly landing, there is normally extensive damage to the UAV's. Belly landings carry the risk that the aircraft may flip over, disintegrate also it can catch fire if it lands too fast or too hard. Extra care should be taken while the UAV lands that is straight and level as possible also it should be having enough airspeed to maintain control over the UAV. The danger of performing belly landing increases with the

involvement of strong crosswinds, damage to the airplane, or unresponsive instruments or controls. Thus here we are designing a suitable parachute for safe recovery of the UAV so as to reduce the kinetic energy of the UAV when it descends and performs landing.

The purpose of a parachute has always been to decelerate and provide stability to a payload in flight. The aerodynamic and stability characteristics of the parachute system are governed by the geometry of the parachute where extreme care is paid to this in the design process. The effects of deployment and also opening forces are critical in the safe operation of the parachute. The opening characteristics play a major role in the selection of geometry and other parameters in the design process. Parachutes for aerospace applications are generally symmetric about the canopy axis. This axis passes through the centre of the canopy and the confluence point of the suspension lines. The canopy is the cloth surface that inflates to provide the desired lift, drag, and stability. The suspension lines are used to transmit the retarding force from the canopy to the payload either directly or by a riser attached below the confluence point of the suspension lines.

Till now various kinds of parachutes have been designed for various applications like pilot, drogue, deceleration, descent, extraction etc. The modelling of the dynamics of parachute is too complex and difficult to be modelled accurately. At the Inflation and the terminal descent stage the dynamics of the parachute are governed by the coupling between the structural dynamics of the chute system and the surrounding air flow.

When the parachute dives in air in steady state the air flowing around the chute will separate at some location on the canopy. The shedding of the vortices from the canopy surface can affect the stability of the system and cause a periodic motion of both parachute and payload. The wake from a porous parachute consists of air that flowed around and through the canopy. The payload body in speed range of the parachute usage sheds a very turbulent wake. The flow entering the parachute is of a disturbed nature and that should also be considered regarding the aerodynamic performance of the parachute. Also for many types of parachutes, this change in airflow can be quite significant to be considered in the time taken by the parachute to inflate. In summary the calculations of different phenomenon involved in parachute like deployment, inflation and also deceleration requires a numerical solution to the equations of motion to the highly unpredictable airflow around which is viscous and turbulent. The parachute is also a flexible body which has a dynamic behaviour coupled with the behaviour of the flow, which passes through and around it. Thus from the above description it is obvious that a full-time solution of this unpredictable system is far from being easily feasible. To make a mathematical model that is feasible, simplifications have to be made, as long as the model can be validated satisfactorily by experiment or by comparison with reference data.

1.1 OBJECTIVES

The main objective of this work is to develop a suitable automatic deploying parachute for the Slybird so that the descent of the UAV can be in a controlled manner without any damage or disintegration of the structure. The project reviews existing circular parachute models and addresses the development of six degree-of-freedom model of a guided circular parachute. The project involves step-by-step development of the mathematical model of circular parachute that includes the basic equations of motion, analysis and computation of the aerodynamic forces and moments. Further it also includes the design for autonomous deployment of the parachute.

The project was completed in two phases where the first phase included a 2 Degree-of-Freedom model .Here the mathematical equations involved in the designing of the model were determined as well as a Simulink model based on the equations was developed.

The second phase comprises of the development of a six degree-of-freedom model of a guided circular parachute, it also involves the autonomous deployment system for the parachute when the UAV is in flight.

The autonomous system developed in the second phase helps the parachute deployment when the free fall of the UAV occurs the system recognizes it and deploys the parachute helping in safe landing of the UAV.

1.2 SPECIFICATIONS

Design requirements and mission specifications of the UAV as well as parachute are:

Table 1.1 Details of Slybird

• Payload	Approx. 4.5 kg (UAV+Chute)
• Range	Around 10 km
• Endurance	45-60 minutes
• Speed	10-30 m/s , 36-108 kmph
• Operating Altitude	30-300m
• Wingspan	1.6m (5.2ft)
• Length	1.3m (4.2ft)

The design of the parachute is based on the design considerations of the UAV, its material properties and others. Following is the required analysis of the strength of the UAV structure.

Considering continuous fibre composite for higher strength and stiffness we have a list of reinforcing fibres commonly used in aerospace applications.

Table 1.2 Reinforcing fibres commonly used in aerospace applications

Fibre	Density (gm/cc)	Modulus (GPa)	Strength (Gpa)	Application Areas
Glass				
E-glass	2.55	65-75	2.2-2.6	Small passenger a/c parts, air-craft interiors, rocket motor casings
S-glass	2.47	85-95	4.4-4.8	Highly loaded parts in small passenger a/c
Aramid				
Low modulus	1.44	80-85	2.7-2.8	Fairings , non load bearing parts
Intermediate modulus	1.44	120-128	2.7-2.8	Radomes, some structural parts
High modulus	1.48	160-170	2.3-2.4	Highly loaded parts
Carbon				
Standard modulus (high strength)	1.77-1.80	220-240	3.0-3.5	Widely used for almost all types of parts in a/c satellites, missiles.
Intermediate modulus	1.77-1.81	270-300	5.4-5.7	Primary structural parts in high performance fighters
High modulus	1.77-1.80	390-450	2.8-3.0	Space structures, control surfaces in a/c
Ultra-high strength	1.80-1.82	290-310	4.0-4.5 7.0-7.5	Primary structural parts in high performance fighters, spacecraft

Given:

Diameter of UAV = 6 inch (approx), 0.1524 meters

Length = 1.3 m

Surface area = $2*\pi*r*h$

$= 2*\pi*0.0762*1.3$

$= 0.6225$ meter^2

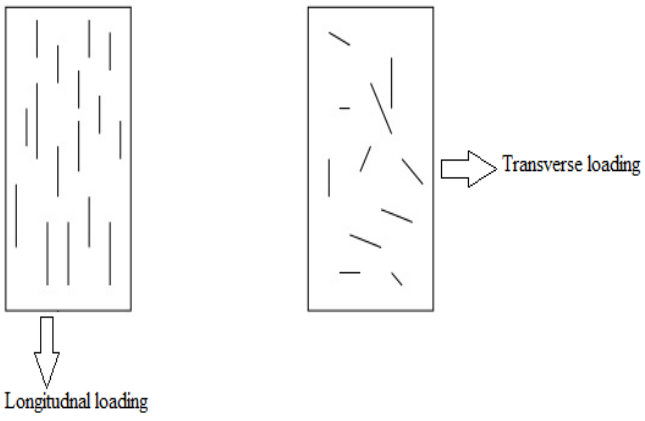

Figure 1.1 Loading in composites

- Longitudinally aligned fibrous composites are anisotropic, maximum strength is achieved in that direction fibre alignment.
- Transverse direction fracture usually occurs at low tensile stress.

As shown in table 1.1 the glass reinforced fibres have a strength of 4.4 – 4.8 GPa i.e. it can withstand 4400 – 4800 N/mm^2. But this strength is when the loading is in longitudinal direction. The strength reduces considerably when loaded in transverse direction and it is as low as 10% of the longitudinal loading. Thus the UAV structure can sustain only 440N/mm^2 in transverse direction.

By the momentum principle, it gives the relationship between the net force on an object and that object's change in momentum

$Fnet = \frac{\Delta P}{\Delta t}$, where $\Delta P = m\Delta v$ m = mass of UAV

$\Delta v =$ Descending velocity

$Fnet = F - mg = \frac{\Delta P}{\Delta t}$

$F - mg = \frac{0 - mv}{\Delta t}$, as final velocity is zero and the initial velocity is in the –y direction as shown in figure 1.2

$= \frac{0-(-4.5*4)}{0.1}$, considering that the time of impact is 0.1 seconds

=180 N

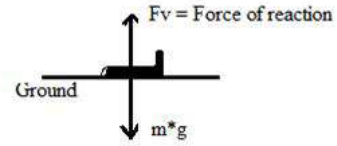

Figure 1.2 Forces on UAV

Thus this is the maximum Impact force which acts on the structure of UAV which is less than the above calculated strength of the UAV structure. From the above it can also be stated as the time of impact increases, further the force induced reduces and thus the landing terrain has an impact on the induced force as grassy land will have more impact time and thus reduces the force acting on the structure of UAV. The force acting on the UAV can be calculated by putting an

accelerometer on UAV and by calculating the acceleration just before it hits the ground and from that the force can be calculated.

Thus from the above it is clear that the force during impact is very less and the air vehicle is safe while landing if the descending velocity is below 4m/sec. The parachute has to be selected and designed based on this velocity. The further chapters give a detailed knowledge about the designing details of the selected parachute.

II. LITERATURE REVIEW

Based on the objectives of the thesis, literature was reviewed. This literature review is the background of the thesis. This section is a discussion of this literature review. For the literature review research papers, sections from books, specifications, standards and regulations were consulted.

2.1 The Aerodynamics of Parachute (AGARD)

This report gives all the details from the very basic of the parachutes designing and other mathematical equations involved in generating the two degree of freedom model design. It emphasizes on the selection of the principal aerodynamic characteristics of parachutes and various known factors which affect these characteristics. It also gives a brief study about the different canopy shapes with their trajectory dynamics and steady as well as unsteady aerodynamics of parachutes.

2.2 Parachute-Payload System Flight Dynamics and Trajectory Simulation

The work traces a general procedure for the design of a flight simulation tool representative of the major flight physics of a parachute-payload system along decelerated trajectories. Here two models are developed and the different parameters of parachute development are considered over them. The major discrepancy between the two models is the level of dynamic stability of the modal response. This has been explained with the extreme sensitivity of the aerodynamic coefficients to centre of gravity location and angle of attack.

2.3 Six-Degree-of-Freedom Model of a Controlled Circular Parachute

The paper provides knowledge over the development of a six-DOF model for a circular parachute that includes the basic equations of motion, analysis and computation of the aerodynamic forces and moments. It also gives the application of the two-step nonlinear system identification algorithm to refine the analytical values of the aerodynamic coefficients based on the available flight test data.

2.4 Notes on Generic Parachute Opening Force Analysis

This report develops a generic opening shock analysis that permits calculation of velocity profiles, shock factors, maximum shock forces and their time of occurrence during deployment for many types of parachutes. Criteria are presented and methods of calculation developed. Application of the analysis to an apparent anomaly in solid cloth parachute finite mass deployment, verifies the parachute diameter effect shown in the test performance.

2.5 A Technique for the Calculation of the Opening-Shock Forces for Several types of Solid Cloth Parachutes

This report gives an analytical method of calculating parachute opening-shock forces based upon wind tunnel derived drag area time signatures of several solid cloth parachute types in conjunction with a scale factor and retardation system steady-state parameters have been developed It also gives the methods of analyzing the inflation time, geometry, cloth airflow properties and materials elasticity are included.

2.6 Observations on the inflation time and inflation distance of parachute

This report summarizes the comments on parachute inflation time and distance from several of the author's previous publications. Additional information is included to explain how recovery systems opening shock forces are determined not only by the specified operational velocity, altitude, and trajectory angle, but are also determined by the initial program requirements of weight, rate of descent, equilibrium altitude, choice of parachute type, and canopy airflow.

Here in this report two accepted axioms on the constancy of inflation distance and the effect of inflation time on the magnitude of the opening shock force are analyzed. The results shown in this report verify that the inflation distance axiom is correct, and that the inflation time opening shock axiom is not correct although it appears to be correct.

2.7 Parachute Decelerate Trajectory Optimization Design Based On Genetic Algorithm

In this paper, the optimal parachute decelerating trajectory of mini- UAV's is studied. The mini-UAV

trajectory model of parachute decelerating segment is established. Here the influences to parachute drag are recognized and the parachute canopy limit area formula is derived. In order to ensure the time effectiveness of mini-UAV's entering working destination, taking flight time and range as the performance function, considering end velocity and end height as optimization constraints, and choosing parachute parameters – canopy area and parachute opening time as design variables, the optimal decelerating trajectory is solved by sequential quadratic programming method and genetic algorithm.

Various other literature reviews were also done so as to get the insight of the parachute opening characteristics, decelerating trajectory and other parameters. Thus here in this report a six degree-of-freedom model of a circular parachute is made over SIMULINK just to get the trajectory generation details and the forces acting in every direction after the parachute is opened full. The results are shown here in the subsequent chapters.

III. KNOWLEDGE GAPS IN EARLIER INVESTIGATIONS

The study of circular parachute modelling has been done over the past years by the researchers. However, a complete model of a circular parachute is still not been developed so far (whereas a number of efficient techniques of the control of maneuverable parachutes like parafoil exists).The other existing higher-degree-of-freedom models of circular parachutes which are uncontrolled lack permissible nonlinear aerodynamics and use mostly empirical values for the apparent mass terms which are being defined by many researchers.

The primary contribution of the work presented here is the development of a six-degree-of-freedom model of a circular parachute with an autonomous deployment system.
The analysis of the circular parachute modelling problem has recognised major two shortcomings in the existing methods that are; estimation of apparent mass terms is done empirically for axis-symmetric shapes and the only aerodynamics considered are only of fully open and symmetric canopies and determining at the opening or closing stages is not possible.
Here in this model of the circular parachute the apparent mass terms are not considered as the height at which the parachute is deployed is very less (nearly15 meters from ground) only, thus those effects over the trajectory of the descending parachute are not remarkable.

Further with regard to aerodynamics of the fully deployed canopies with a symmetric shape, many authors have proved that the nonlinear basic aerodynamic terms are a function of the angle of attack. For instance in ref[20] authors discuss parameter identification using flight test data, where they point towards that the dependence of aerodynamic terms on the angle of attack is highly nonlinear unlike those of an aircraft. Many other papers [8,17,18,19] provide sufficient data for fully deployed canopies and variety of flight conditions. (Similarly to the aircraft aerodynamics the majority of data which is available has been obtained on the basis of wind-tunnel experiments). The aerodynamics of a distorted canopy has not been considered. In summary the consensus on the lack of accurate dynamic modelling of apparent mass effect and nonlinear dynamics of distorted canopies has been emerged.

IV. SCOPE AND OBJECTIVES OF PRESENT PROJECT

The project aims at Slybird, a mini-unmanned vehicle developed by National Aerospace Laboratories having its primary users to be police and military. The UAV has landing problems on different terrains because due to belly landing it tends to disintegrate at any harsh landing conditions. Thus for this problem here in this project a parachute is designed for the UAV such as to provide it a softer landing condition and reducing the chances of its disintegration.

The project aims at building a six degree-of-freedom model of the circular parachute which gives us the knowledge about the trajectory of the descending parachute with the UAV. Based on the trajectory generated we can find out the region from the point of parachute deployment to which it would land on the ground as well as the vertical and horizontal velocity profiles can be generated. The roll, pitch and yaw angles can also be closely seen so that the control of the parachute can be accomplished.

The project introduces an autonomous deployment system based on an Arduino microcontroller, using sensors to determine the GPS coordinates acceleration and the battery voltage of the UAV. When the system determines that the UAV's battery has depleted, or that it is operating outside prescribed boundaries defined by GPS, or that the whole unit is under free fall, the recovery system cuts power to the motors and deploys the parachute, thus helping the UAV to descend to the ground safely at a permissible velocity without any harm to the UAV.

The above system is well defined in the following chapters keeping in mind the different design considerations. The project starts with a brief introduction to the two degree-of-freedom model and then continues to the six degree-of-

freedom model of a circular parachute. Further the recovery system is explained elaborately with other designs and graphs presented in a manner such that the mathematical Simulink model and the graphs are self-explanatory.

V. PROBLEM DEFINITION

The problem was to design a suitable recovery system for the mini un-manned aerial vehicle which helps the system to land safely without any harm to the UAV.

The project mainly focuses on the development of the parachute system for safe landing of the UAV which generally undergo belly landing and because of the landing at uneven surfaces they generally get disintegrated. So as to save UAV from being damaged and helping it to land at any surface with less loss to its structural strength an autonomous deploying parachute system was to be developed so that it can be controlled remotely or with the help of sensor data it can sense and deploy the parachute whenever it is required during the flight of the UAV.

Since the UAV has a low range of flight that is it does not attain much height while flying and when the parachute opens it is not having much height from the ground, so we cannot design a controlled parachute system here which can control the trajectory of the falling system as predefined by the operator. Thus here the parachute designed is not a controlled parachute because controlling the parachute requires some endurance in height so that at least the system gets time to analyse its position and the error from the desired trajectory as given by the operator and then process so as to reduce the incoming error. The deployment and the landing of the system on the ground do not take more than 10 -15 seconds, and doing anything to control parachute is difficult in this span.

Thus the parachute system designed here gives good results in simulation over SIMULINK. The wind effects can also be taken into consideration and the effects over changing trajectory can be seen in the 3D-plot. The Six Degree-of-freedom model described here can be utilised to manufacture an autonomous recovery system for UAV's and thus the problem defined above can be solved.

VI. METHODOLOGY FOR SOLUTION

The project was divided into two phases; the first phase included analysing the problem definition and developing a basic mathematical model of a two degree of freedom model using Simulink. Analysis was made over the design parameters of the parachute and the deployment system parameters.

The second phase included development of a six degree of freedom model based on the analysis done during the first phase. The further mathematical analysis was made over the calculation of centre of mass of the whole system and then transferring the moments of inertia of different parts to this mass centre and then generating equations so as to develop the model in Simulink.

The second phase also includes the development of the autonomous recovery system using Arduino Nano Microcontroller which is coupled with Accelerometer, GPS, Servo motor and other equipments. The recovery system is so designed that it works to monitor three conditions to determine if aircraft failure has occurred: main battery voltage of UAV getting depleted, free fall of UAV and getting away of UAV from the defined GPS coordinates.

PHASE – I

The study starts with the basic knowledge of the parachute and the mathematical equations involved in the designing of a suitable parachute for the UAV.

6.1 Aerodynamics of parachute at the steady state

To start with the aerodynamics of the parachute we first here describe the filling of air in the parachute canopy which is termed as the inflation process and also the opening of the parachute from its bag which is also known as the deployment process. After all these processes are explained we will move towards its falling trajectory generation that is how the parachute is coming down or decelerating and finally we look forward towards the steady state. The basics of the parachute concepts of its aerodynamics are introduced by firstly considering its steady state descent after it is fully deployed.

Here we start with the determination of the axes of the parachute that is its body axes and the ground axes and then by using the transformation matrix the parameters like velocity, acceleration and others are determined in the body frame with respect to the ground. The assigning of the axes is based upon the forward direction motion of the vehicle which is to be determined first. After the forward direction of motion is analysed then the orthogonal set of axes which fixed with the vehicle, and which passes through the origin which itself has been fixed on the vehicle and these fixed orthogonal set of axes are referred to as the body axes.

In the figure below it is shown that the axis O-X is so positioned that it is pointing in the forward direction with the parachute canopy movement. In figure 6.1, the α is the angle of attack which is measured between the airflow direction V, in the OXZ plane with the OX axis which is also the body axes in the forward direction which is represented in the figure given on the next page.

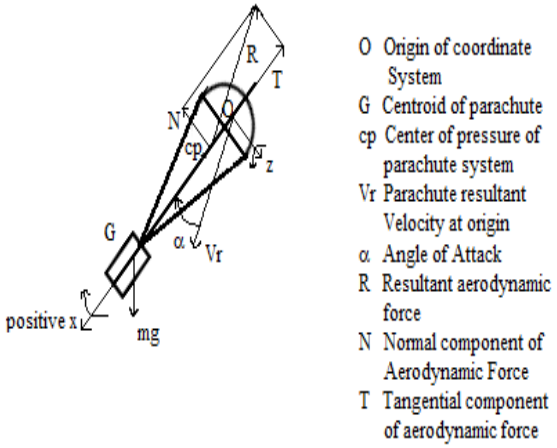

Figure 6.1 Body axes with components of force.

Parachutes are like any other body which is submerged in fluid, which here is air. When the parachute moves in fluid that is air an aerodynamic force gets developed over it which is represented here as R. This force and the resulting moment at any location, due to this resultant force can be measured experimentally. The resultant force value can be determined by the experiments but they do not help in determining the center of pressure position which is precise enough where the force can be analyzed that it would act at a particular point on the line of action. For determining actually that where the center of pressure is on the canopy, the intersection of the line of action of the calculated aerodynamic resultant force is considered with the axis of the symmetry of the canopy or chute.

The Drag force produced on the parachute due to the resistance provided by the chute canopy to the airflow has been considered to be the most significant characteristic of the parachute development. In other words it is the component of the aerodynamic force in the direction of the airflow or the velocity of the air Vr, and also the other force in the plane of this velocity is the aerodynamic lift force that is L.

The other components of this aerodynamic force, one in parallel direction to the O-X axis is called the tangential force T, and the other in normal direction to the O-Z axis is the Normal force and these two components of the resultant aerodynamic force can be expressed as in equations 6.1 and 6.2 which are:

$$C_{Tan} = T / (1/2\rho Vr^2 So)$$
$$C_{Nor} = N/1/2\rho Vr^2 So \quad (6.1 \&6.2)$$

In the above equations, the ρ is being defined as the local air density, or the density of the surrounding fluid. Vr, is the resultant velocity of the parachute at the origin of the coordinate system as defined above which is told to be fixed with the parachute system and finally So, can be defined as the total surface area of the canopy which also includes any kind of opening, or vent area for the better steering of the parachute which will be defined earlier.

The C_{Tan} and C_{Nor} depend solely upon the density of the air flowing around, its viscosity and also the temperature. Then by the dimensionality check we have,

C_{Tan} and C_{Nor} = f (□□□Re; Ma) (6.3)

Where, $Re = V_R Do/v$ is the Reynolds number

And,

$$Do = [4So/\pi]^{1/2} \quad (6.4)$$

Where, the nominal diameter of the parachute as calculated is denoted by the letter Do, and the kinematic viscosity of the flowing fluid is given here as v.

Here the Mach number is also considered and is represented as $Ma = V_R/a$. The local speed of sound in the fluid which is also undisturbed is given here as .

The figure below gives the relationship between the coefficients as defined above:

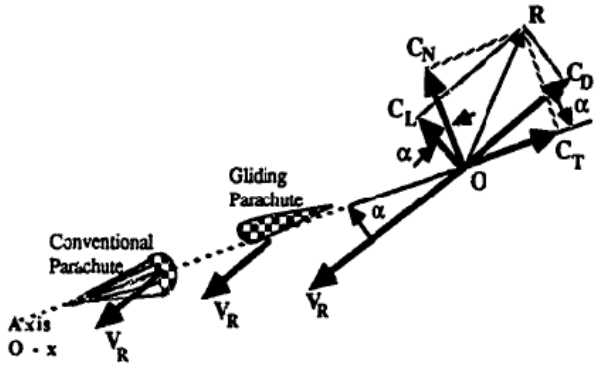

Figure 6.2 Showing the relationship between the C_{Tan} and C_{Nor} with C_{Drag} and C_{Lift}.

$$C_{Drag} = C_{Tan}\cos\alpha + C_{Nor}\sin\alpha \quad (6.5)$$

$$C_{Lift} = C_{Nor}\cos\alpha - C_{Tan}\sin\alpha \quad (6.6)$$

$$C_{Tan} = C_{Drag}\cos\alpha - C_{Lift}\sin\alpha \quad (6.7)$$

$$C_{Nor} = C_{Lift}\cos\alpha + C_{Drag}\sin\alpha \quad (6.8)$$

6.2 Changes in Coefficients with the Reynolds Number

There are many papers available on the change perceived in the aerodynamic coefficients with the changing Reynolds number. The reference [2] gives the variation which is mainly concerned with the variation of the drag coefficient. In different researches it is also proved that the Reynolds number which is based up on the canopy nominal diameter of the parachute as defined above is greater than 10^5. The figure 6.3 shows this change on the aerodynamic coefficients with the changing Reynolds number.

In figure 6.3, the achieved data is also being compared with the other body data which is collected when the Reynolds number is changed when the flow occurs over them. The two bodies considered here are the sphere and a circular disc which are placed normal in the flow. From the figure it is proved that at high Reynolds number the boundary layer over the body gets separated from the surface of the body and also closer to the leading edge of the body the separation of the flow occurs.

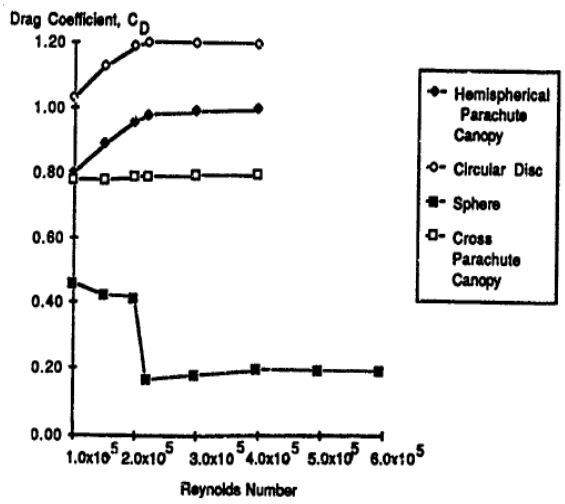

Figure 6.3 Effect of change in Reynolds number over the Aerodynamic coefficients.

Thus from the above figure it can be shown that there is very less variation in the boundary layer occurs with the changing Reynolds number. In figure 6.4 the variation is shown for the flat circular canopy.

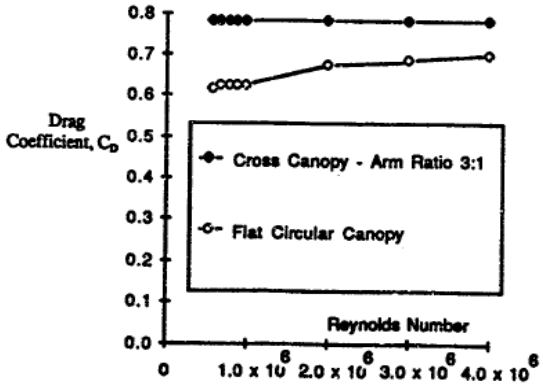

Figure 6.4 Effect of change in Reynolds number on Cross and Flat Circular canopy ref [2], [3]

6.3 Equilibrium state mechanics of parachute

So as to define the mechanics of the parachute system the basic formulas are used. First the free body diagram is made showing only the forces acting on the system. For the system shown in figure 6.5, the forces acting are being resolved and the moments of these external forces are calculated, after which the condition for the equilibrium of the parachute system is achieved. Here, in the figure the angle θ is shown as the incline of the chute axis of symmetry, with the vertical. At this moment, the drag force acting over the canopy has been considered to be minimal or negligible.

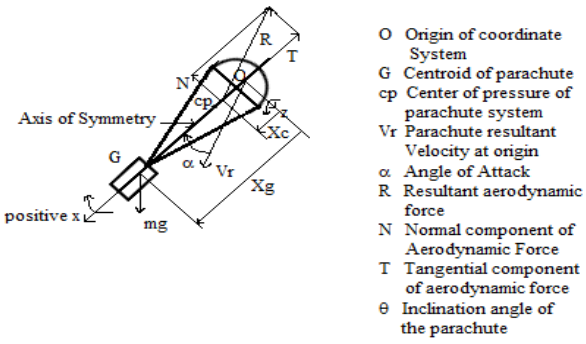

Figure 6.5 Free body diagram of the Conventional Parachute

Finding components in the O-X direction

$$mg\,(\cos\theta) - T = 0 \quad (6.9)$$

Components in the O-Z direction

$$mg\,(\sin\theta) - N = 0 \quad (6.10)$$

Calculating moments around the centroid of the system, G

$$M_G = -N\,(Xg - Xc) = 0 \quad (6.11)$$

From the above equation it is inferred that we cannot have (Xg – Xc) as zero, so we can only have N to be zero for equilibrium condition.

Further in the study it can be said that the equation 6.10 represents that the weight of the system since it will never be zero, so when during equilibrium condition the angle θ must have the value zero.

From the above discussion it can be seen that when in equilibrium condition the parachute descends having its axis of symmetry in vertical direction and also with angle of attack α so that the normal aerodynamic component of force is not developed on the system.

The Flat Circular parachute is the cheapest to be utilised for small application as required here in this project. These are mostly used as devices used to produce drag so that the payload can have a safe landing and also they do not provide any lift force as with the gliding parachute where the lift force produced is controlled by controlling the control lines by the glider. The circular chutes are mainly the drag producing devices used in military and other applications where the payload is to have a safe landing.

The chute is made up of cloth which is in triangular forms and each part is called as a gore. The chutes developed in the olden days had instability issues as they were simply developed. The further improvement for these round parachutes included making hole at the top where all the gores are attached so that the air which is getting accumulated inside the canopy is released from there. This was being done because the filled air tried to escape from the canopy and thus it tried to carry the canopy with itself and thus there were oscillations in the canopy and so as to reduce these oscillations about the axis of symmetry, the hole was made at the apex. The parachute having no hole at the apex has greater chances of getting oscillations while descending. So as to make the round chutes steerable researchers have proposed to make cuts along the gores so that the air can escape from the cut portion providing a velocity to the chute in the opposite direction. Thus these chutes can also be controlled using different control techniques.

The figure 6.6 represents a circular canopy. The model was made using designing software like Solidworks. The work conducted in future of this report is development of a Simulink model over which we will simulate the parachute system.

Figure 6.6 SolidWorks model of the Canopy

VII. PROBLEM FORMULATION

This section contains a study about the 2 degree-of-freedom model of the parachute system. In this section calculations about the opening shock factor as well as the maximum force acting during deployment are formulated. The

aim of this part is to find out the forces during opening of the chute or the shock generated when the chute is deployed, for the flat circular parachute to be developed. Further the model is also made in Simulink and the other parameters are also calculated henceforth.

For the analysis of the problem here we start with considering the problem in view of the laws of motion given by Newton. Constant mass condition is considered here as the mass is not changing for the system, so as to simplify the given problem with the consideration that the parachute opens horizontally. The equation given in reference [4] helps us to derive the relationship between the ratios of drag area with the chute velocity, which in the end gives the value of the shock generated at the instant when the parachute opens. Also the force generated as the shock force as well as the maximum force in the different mass conditions state that is for finite, intermediate also the infinite mass range is generated.

7.1.1 Motion equation at the opening phase of chute.

The problem starts with the very basic model where we are just considering a simple mass system having a point mass which is just having the weight of the system as a force and the pull of the chute generated due to the drag from the canopy as shown in the figure 7.1. The analysis is carried out in the horizontal form and the forces are represented as in the figure.

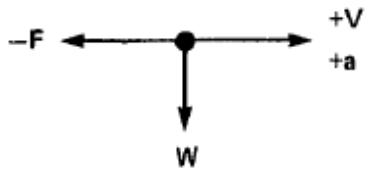

Figure 7.1Force system considering chute as a point mass

-F = ma

$$-\frac{1}{2}\rho v^2 C_{Drag} S = \frac{w}{g}\frac{dv}{dt}$$

$$\int_0^t C_{Drag} S dt = \frac{2W}{g\rho}\int_{v_S}^{V}\frac{dv}{(-v^2)} \qquad (7.1)$$

The above equation in 7.1 can now be simplified by multiplying this given term on the right hand side of the equation.

$$1 = \frac{C_{Drag} S_o t_o V_s}{C_{Drag} S_o t_o V_s}$$

After the multiplication the equation generated is suitable for the analysis of the parachute system and the previous equation in 7.1 becomes,

$$\frac{1}{t_o}\int_0^t \frac{C_{Drag} S}{C_{Drag} S_o}\, dt = \frac{2W}{\rho g C_{Drag} S_o t_o V_s} V_s \int_{v_S}^{V}\frac{dv}{(-v^2)} \qquad (7.2)$$

7.1.2 Ratio determining the different mass conditions for parachute

$$\text{Let H} = \frac{2W}{\rho g C_{Drag} S_o t_o V_s}$$

The ratio defined above is termed as the ratio of the mass, which describes the condition which is to be considered for the finite, intermediate or the infinite mass condition. This ratio defined here is discussed in detail in reference [5]. The correctness of this analysis of the chute deployment calculation depends on the correctness of the different parameters.

Equation (7.2) represents here the accurate mathematical description of the dynamic ratio of the drag area ($C_{Drag}S/C_{Drg}S_o$) and also the inflation distance (Vs*to) are necessary for reliable calculations. Various methods generated for the calculation of shock-force at the opening are also based on the formulae s if there was single solution only.

The solution to the equation 7.1 as defined earlier in the text for the condition that the chute is open full and is retarding that is it is having the constant $C_{Drag} S_o$, and from this the ratio of the velocity is given as,

$$\frac{V}{V_s} = \frac{1}{1+\frac{\rho g C_{Drag} S_o t_o V_s}{2W}} = \frac{1}{1+\frac{1}{H}} \qquad (7.3)$$

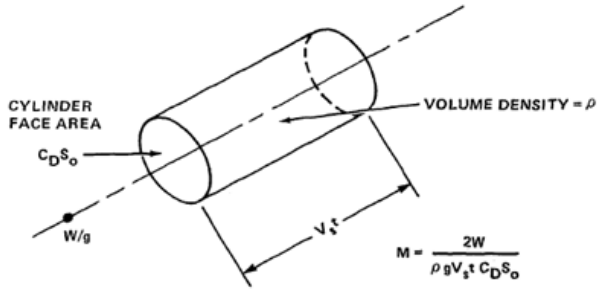

Figure 7.2 Mass ratio concept

Here it can be shown that the mass of air entering the cylinder is changing at each instant and with every instant the ratio of the velocities associated with the defined ratio of mass is also changing

7.1.3 Analysis of the general deployment procedure

Here we can say that the ratio of the mass H, is developed in the equation automatically and which also interacts with the different parameters of the parachute which define its geometric as well as the different aerodynamic properties. Thus it is proved that it is the best parameter to switch between the different mass conditions. Thus from the equation 7.2 we have,

$$\frac{1}{t_o}\int_0^t \frac{C_{Drag}S}{C_{Drag}S_o}\,dt = HV_s\int_{V_S}^{V}\frac{dv}{(-v^2)} \tag{7.4}$$

Further we integrate the term on the right hand,

$$\frac{1}{t_o}\int_0^t \frac{C_{Drag}S}{C_{Drag}S_o}\,dt = H\left(\frac{V_s}{V}-1\right)$$

Then velocity ratio is give as,

$$\frac{V}{V_s} = \frac{1}{1+\frac{1}{Ht_o}\int_0^t \frac{C_{Drag}S}{C_{Drag}S_o}dt} \tag{7.5}$$

Thus the force generated at any given time instant is te drag force given as,

$$F = \frac{1}{2}\rho v^2 C_{Drag}S,$$

Also from above it can be stated that the drag force generated at the velocity of deployment (Vs) is,

$$Fs = \frac{1}{2}\rho V_s^{\,2} C_{Drag}S_o,$$

Now the ratio of the equations above that is $\frac{F}{F_s}$ is termed as the shock factor at an instant or the instantaneous shock factor, denoted by Zi

The ratio F/Fs is the instantaneous shock factor, Zi

$$Zi = \frac{F}{F_s} = \frac{\frac{1}{2}\rho v^2 C_{Drag}S}{\frac{1}{2}\rho V_s^{\,2} C_{Drag}S_o}$$

$$Zi = \left(\frac{V}{V_s}\right)^2 \frac{C_{Drag}S}{C_{Drag}S_o} \tag{7.6}$$

As during the test in the wind tunnel the velocity and the density remain constant when the infinite mass condition of deployment is considered,

$$Zi = \frac{F}{F_s} = \frac{C_{Drag}S}{C_{Drag}S_o} \tag{7.7}$$

Thus the shock factor Zi described above is in accordance with equations 7.5 and 7.6,

$$Zi = \frac{\frac{C_{Drag}S}{C_{Drag}S_o}}{\left[1+\frac{1}{Ht_o}\int_0^t \frac{C_{Drag}S}{C_{Drag}S_o}dt\right]^2} \tag{7.8}$$

From this equation above, we can also find out the time of occurrence of the shock force which is maximum by just differentiating the above shock factor equation Zi with respect to time and then putting that equal to zero we achieve,

$$\frac{dZi}{dt} = \left[H+\frac{1}{t_o}\int_0^t \frac{C_{Drag}S}{C_{Drag}S_o}\,dt\right]\frac{d\left(\frac{C_{Drag}S}{C_{Drag}S_o}\right)}{dt} - \frac{2}{t_o}\left(\frac{C_{Drag}S}{C_{Drag}S_o}\right)^2 = 0 \tag{7.9}$$

The shock factor equation defined above has been equated to zero, and the maximum shock factor Zi, generated can be given by putting the value of the ratio of time (t/to) in the equation 7.8. Since this mass ratio defined above gets increased from a very lower value so the maximum force generated and also the time of occurrence is calculated after

the shock force develops in the inflation process. The mass ratio is the minimum or the limiting one at t=to, that is when the shock force becomes maximum at the time instant *to* which can be given as H_L, for the finite mass condition. Further when this ratio of the mass is increased it results in the occurrence of maximum force after the *to*, which is the inflation reference time for the canopy which is also much less as compared with the infinite mass ratio condition. As the time passes, the gradual increase in the mass ratio, H results in the infinite mass condition opening shock force.

In the equation 7.9, given above the term $\frac{d\left(\frac{C_D S}{C_D S_o}\right)}{dt}$ defines the inflation rate of the parachute .It is the general equation defining the inflation time taken by a parachute. The parachute cloth also has some porosity so the inflation of the chute starts slowly and after some time it gains a constant rate of inflation, unless the parachute is fully-open for the first

time after which the area produced for drag limits itself in the process and the inflation rate starts to decrease, and in the process further it reduces to zero, also for the maximum drag area ratios given in the range 1.05 to 1.1, which gives us the range of the infinite mass opening shock factor Zi. Also if we use the solid cloth canopies with low or no porosity present the inflation rate increases continuously.

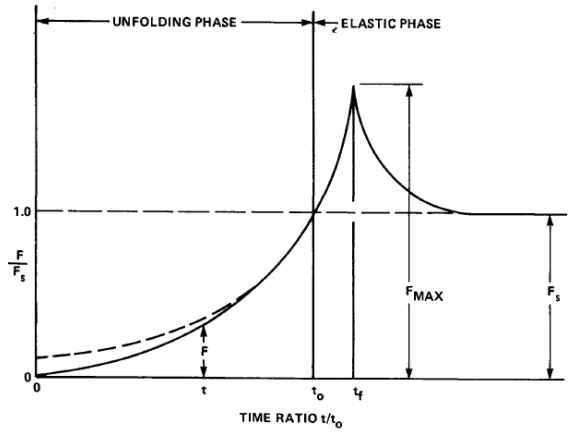

Figure 7.3 Figure showing the opening forces for solid cloth parachute

7.2 PARACHUTE SELECTION

From the above it is made clear that the type of parachute used for the Slybird is a flat circular parachute because the height at which the UAV dives is less and the parachute has to be opened at a very less height away from the ground. The control of the parachute can only be done here by cutting vents across the canopy cloth and not by the control of suspension lines as in the case of Ram air type parachutes. Thus the design parameters of the flat circular parachute are given as below and in further chapters the two and six degree-of-freedom models are illustrated.

Here we have the calculation for the diameter of the desired parachute.

$$C_D S_o = \frac{F_D}{0.5\ \rho V^2} = \frac{mg}{0.5\ \rho V^2};$$ At equilibrium condition (7.10)

Where,

m = 4.5 kg (Mass of UAV + Mass of parachute)

g = 9.81 (acceleration due to gravity)

ρ = 1.225kg/m^3 (density of air, taken to be constant at low altitudes)

V = 4m/sec (safe landing velocity for the Slybird)

C_{Drag} = Coefficient of drag (0.7 for flat circular parachute according to Knacke [6])

So = Parachute area or the required area of the parachute to produce the desired drag

Calculating,

$C_{Drag}S_o = (4.5*9.81*2)/ (1.225*4^2)$

$= 4.504\ m^2 = 48.48 ft^2$

Calculating the nominal diameter, we have

$$D_o = \sqrt{\frac{4S_o}{\pi C_D}} \quad (7.11)$$

$Do = \sqrt{\frac{4*4.504}{\pi*0.8}}$ = 2.68meters or 8.8 feet ~ 9feet

Thus from the above calculation the nominal diameter of the parachute comes out to be 8.8 feet which can be approximated well to 9 feet.

- Length of Suspension line

L_S = Canopy diameter * C_D

= 9.0* 0.8

= 7.2 feet

For the safe opening of the parachute from the bag placed over the UAV it is to be pulled out by some mechanism at a distance which is equal to the four or six times the diameter of the UAV

- Canopy Inflation time

From Empirical methods we have the equation as,

$$t_f = \frac{nDo}{v} \quad (7.12)$$

Where, the inflation distance was expressed as '*n*' multiples of the canopy diameter Do.

The inflation time was calculated as the time needed to traverse that distance travelling at the deployment velocity *v*. Much analysis over canopy inflation time is given in reference [6].

Here,

n = 8 (fill constant for solid cloth parachute [7])

t_f = (8 * 2.68)/ 12

t_f = 1.8 seconds

- Estimation of the expected load on the parachute

After we have calculated the size required for the parachute with the knowledge of the dynamic pressure and the payload characteristics the maximum force which can act over the parachute canopy can be calculated as given below,

$$F_{max} = q_{deploy} (C_D S) C_i Z_i \quad (7.13)$$

Here,

F_{max} = maximum expected load

q_{deploy} = pressure generated at the time of initiation of deployment process

$C_D S$ = drag area generated by the fully open canopy of the parachute

Zi = Opening shock factor

Ci = factor for the reduction of force

Zi is the shock factor at the time of opening (or can also be considered as the added mass factor which can be understood as the mass of air which moves with the parachute when it descends slowly to the ground.) is used to account for dynamic loads that results from the starting inrush of air and its momentum when canopy initially opens. This can be calculated using the mass ratio concept as explained earlier in the report.

Ci is taken here as the force reduction factor to take care for the reduction in the forces after the inflation process has completed. This can be explained as when the parachute with the payload descends there is some drag force also produced on the payload and it slows to a minimum value until the canopy of the chute fully opens, thus by this time the values of the dynamic pressure and the velocity decreases to a very small value as compared to their values considered at the time of beginning of inflation process

$$X_i \approx 0.1 \qquad Xi \approx \frac{W}{C_D S_0} \quad (7.14)$$

Dynamic Pressure

$$P_d = \frac{\rho v^2}{2} \quad (7.15)$$

$= (1.225*12^2)/ 2$

= 88.2 Pascal

= 1.8522psf

Now the maximum force is

$$F_{max} = q_{deploy} (C_D S) C_x X_i$$

= 1.8522(48.48)1.1*0.1

= 9.87 lbf

= 43.9 Newton

By this we have the maximum force generated at the time of opening of the parachute. The UAV structure should be strong enough to bear this instantaneous load which reduces as the canopy gets fully opened.

- Strength of the cloth of canopy

The strength of the cloth used for the canopy is given by the simple membrane theory which is defined elaborately in reference [6]. The strength calculated for the cloth is based upon the assumption that the canopy after inflation gets a spherical shape and the maximum shock force acting on the canopy also occurs at the time of fully open canopy or at the maximum diameter of the parachute.

$$t_c = \frac{F_{max}}{\pi D_p} (D.F) \quad (7.16)$$

Where,

t_c = strength of the fabric required (force/ unit width)

Dp = maximum diameter of the canopy when it is fully open.

D.F = appropriate design factor (6-10)

$t_c =$ 9.87 * 6 / (π *3)

$t_c =$ 6.28 lbf/inch

After the calculation of the fabric strength and the maximum force generated the suspension lines can be designed where the number of lines required to hold the maximum force generated would be the min design consideration.

$$B.S_{S.L} = \frac{F_{max}}{n_{S.L}}(D.F) \quad (7.17)$$

= (9.87*6)/ 16
= 3.7015 lbf or 16.45 Newton

The two degree of freedom model as described above is implemented in SIMULINK with the figure below showing the actual model. There were various assumptions in describing the two degree-of-freedom model. Further the six degree-of-freedom model is explained.

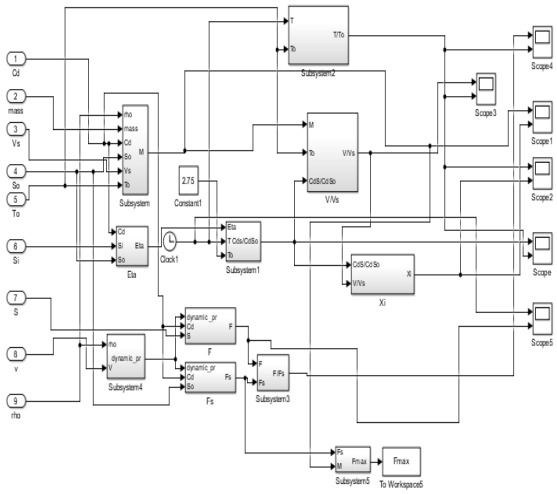

Figure 7.4 Simulink model of the two degree of freedom system of parachute

The model generates all the desired graphs and illustrates the maximum opening force as well as the parameters affecting the stability of the parachute. The two degree of freedom
model cannot be treated as the final result as the various parameters like moment of inertia, added mass, fluid structure interaction and other parameters are yet to be calculated. This just gives knowledge about how the parachute will behave or its unfolding phase and the elastic phase.

Thus further elaborated study was done over the six degree-of-freedom model for the parachute and the results generated from that model are only discussed after that in the following sub-sections

PHASE II

Here in this phase we are developing the six degree-of-freedom model which contains the various equations involved in the development of the model. This section also describes the problems arising in the development of the model. The section here begins with the motion equations which is followed by the calculation of the aerodynamic forces with the moments and concludes with the Simulink model of the derived equations which clearly explain the trajectory followed by the desired parachute as described above. The structure of the parachute system built can be as shown in figure 7.5. To move in the different frames of reference here we consider a body frame and the fixed frame on the ground. A transformation matrix is also used in the Simulink model which can convert from one frame to the other frame.

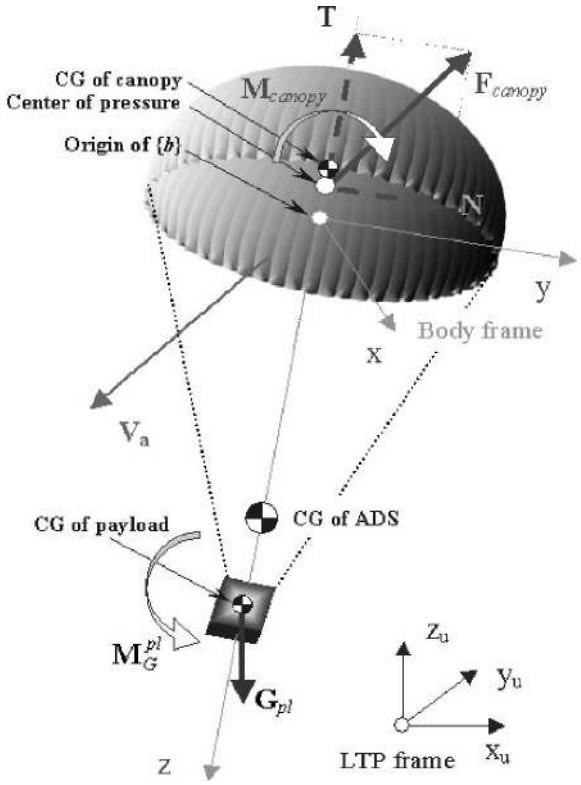

Figure 7.5 System of axes for the desired parachute system

The coordinate axes considered are as shown in the fig 7.5. Here the parachute system shown has its linear position which is considered with the local orthogonal axes which is placed on the ground or can be stated as the ground reference frame that is {u}. The NER coordinate system is also followed here that is the positive y direction gives the direction of the local North, also the positive X direction as shown in the figure points in the eastward direction and the z

direction is upwards or in the axis of symmetry of the system. The payload here shown is just a indicative of the UAV which would be further incorporated in the study. This is being done so as to simplify the problem considered.

Further the other calculations are performed in the coordinate frame which is fixed on the body that is {b}. The coordinate frame of the body has its origin at the open end plane of the parachute canopy which is as shown in the figure. From the figure we can also see that the X and Y lie almost parallel to the canopy's base plane and the axis Z is aligned with the axis of the parachute which passes through the centroid of the payload attached to the system.

The origin of the frame {b} can also be placed at the centroid of the canopy but to determine this location it is very difficult but various research papers publish the origin of the body frame at the centroid of the canopy only. When the canopy is fully inflated it takes the shape of an ellipsoid rather it can also have different ratio of major and the other minor axes because of this reason we are not having a particular formula to calculate the centroid position of the formed ellipse and further we cannot also define the correct place of the Z coordinate.

The following assumptions mostly adopted from the Tory and Ayres paper [8] were used to develop the model:

- "Due to the predetermined architecture the parachute and also payload are considered to be rigidly bounded with each other."
- "At the time of air drop, these two connected parts are assumed to have only gravity force and the aerodynamic forces. Here in the model we are also considering wind effects."
- "The canopy has a center of pressure at which it experiences all the aerodynamic forces and its moments."
- "The aerodynamic forces which get generated because of the payload are taken to be negligible."
- "The canopy when it is undisturbed has an axial symmetry about the z axis."

It is also considered that when the parachute deploys the UAV has no control over the trajectory generated and the motors on the UAV are switched off.

7.3 Geometry of the considered Parachute System

The parachute geometry consists of the payload , suspension lines and the canopy. These three parts constitute the whole system. On the figure it is represented that the distance of the centroids of these parts with the origin of the body frame which is shown as point O in the figure 7.6.

On this figure Rp = $\frac{2}{3}$Ro, represents the chute inflated radius. Here the payload considered is a square block of the same mass as the Slybird and is having all the dimensions similar to a_{pl}, this has been done so as to simplify the problem as determining the actual centroid of the UAV was difficult at this initial stage of design.

From the above explanation it is seen that the shape of the canopy after the inflation has occurred is similar to the hemispheroid which can also be explained as when the inflated canopy is seen from the bottom face or the top face or from the Z axis it appears to be in circular shape and appears to be in ellipse shape when seen from the front plane. The generated Solidworks Model is shown in the figure below with all the notations of the centroids of the system. Here ε is defined as the ratio of the canopy's minor to major axes.

From reference [8] we can say that this ratio for our flat circular canopy is mostly considered to be nearby 0.5. Also some of the other researchers have taken it to be equal to 1 but for the parachute system considered over here the value is taken to be equal to 0.8.

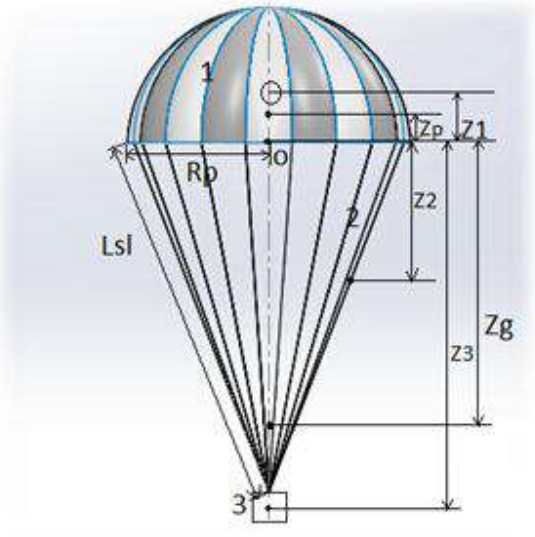

Figure 7.6 Parachute system geometry

7.4 Calculation of the Moments of Inertia for the different parts of the system

Here to move forward we have to first define a mass center of the whole system at which the moments of inertia

from the each part of the system can be calculated. The determination of this point over the system generally requires the knowledge of weight and the shape or dimensions of the components.

At first so as to find out the moments of inertia from each component we have to find out the distance of the centroid of each component with one of its surface z_i as well as the moments of inertia of the respective components with their corresponding centroids is determined as shown in the figure below.

Table 7.1 gives the formulas for each component. Figures 7.7a – 7.7c show the components. Although formulas for a hemispherical shell and payload are known as given in reference [9], the formulas for a hemispheroidal shell and for a frustum right circular cone shell formed by suspension lines are given in the table below.

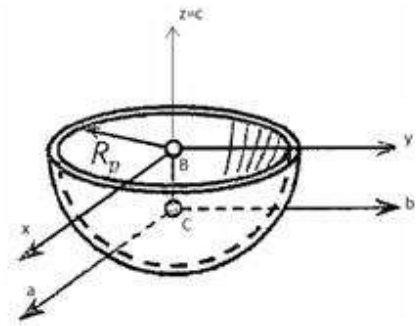

Figure 7.7 (a) Canopy diagram

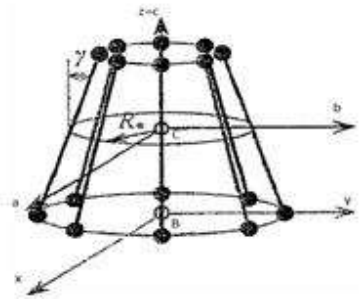

Figure 7.7 (b) Figure showing Suspension lines

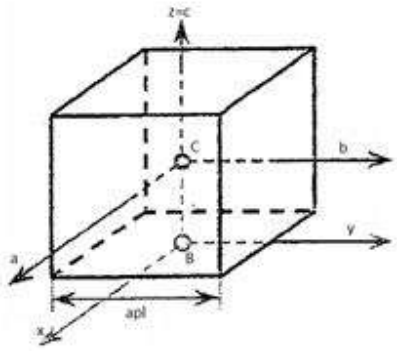

Figure 7.7 (c) Considered Payload system

Table 7.1 Formulas for Moment of Inertia for parachute components

Component	z_i=|BC|	$I_{xx}=I_{yy}$	I_{zz}
Canopy	$\frac{-Rp}{2}\varepsilon^{0.83}$	$0.246m1Rp^2e^4$	$\frac{2}{3}m1Rp^2(1+0.143ln\varepsilon)$
Suspension line	$\frac{Lcos\gamma}{2}$	$\frac{m_i}{2}\left[\frac{L^2(1+cos^2\gamma)}{12}+R_\#^2\right]$	$m_i\left(\frac{L^2sin^2\gamma}{12}+R_\#^2\right)$
Payload	$\frac{a_{pl}}{2}$	$\frac{m_4a_{pl}^2}{6}$	$\frac{m_4a_{pl}^2}{6}$

In Table 7.1 $R_\#$ is the radius of the generated shell measured at the z coordinate of the centroid which can be given as,

$$R_\# = R_p - L_{sl}\,sin\gamma/2 \tag{7.18}$$

The cone formed at the full inflation of the canopy has the angle γ as the half of the angle for the parachute system considered and it can be calculated from the formula given below in equation 7.19.

$$sin\gamma = \left(R_p - a_{pl}/\sqrt{2}\right)\Big/ L_{sl} \tag{7.19}$$

After the computation of the individual moments of inertia these were to be transferred to the frame {b} origin or to the origin of the body frame which was done using the parallel axis theorem as shown below,

$$I^i_{jj} = I^i_{jj} + m_i z_i^2\,, \qquad i = 1...,3 \tag{7.20}$$

Finally the total Moment of Inertia was being calculated for the whole parachute system from the corresponding formula.

$$I_{jj} = \sum_{i=1}^{3} I^{i}_{jj} \quad (7.21)$$

Thus here it can be noted that the major contribution towards the moment of inertia into Ixx and Iyy is maximum by the payload and the moment Izz is mainly controlled by the parachute itself and in this the payload has a very less influence

7.5 Total aerodynamic forces on the stable canopy

The forces and their moments as shown in the figure 7.5 are present because of the force of air and as well as the weight of each component. Thus it can be written as

$$F_{total} = F^{a/d} + G, \qquad M_{total} = M^{a/d} + \sum_i M^{i}_{G} \quad (7.22)$$

Where,

$$G = {}^{u}_{b}R^{T} \begin{bmatrix} 0 \\ 0 \\ mg \end{bmatrix}^{T}$$

(The apparent masses if considered they do not contribute to the weight of the system, here these masses are not considered due to design considerations.)

The other unknown parts of the equation 7.22 are given as below:

$$F^{a/d} = F_{Canopy} + F_{risers}, \qquad M^{a/d} = M_{Canopy} + M_{risers} \quad (7.23)$$

For the calculation of the model parameters the initial values of the various coefficients were required which were taken from the two research papers from Knacke [11] and Moseev [12].

The papers also define the dependence of the various aerodynamic coefficients over the angle of attack which is as shown in figure 7.8

In this figure 7.8 C_D (α_{sp}) denotes aerodynamic drag coefficient and C_M (α_{sp}) denotes the whole system moment coefficient where both of them depend upon the spatial angle of attack. This is used in the generation of the Simulink model as these coefficients control the various pitch, roll and yaw movements of the whole system

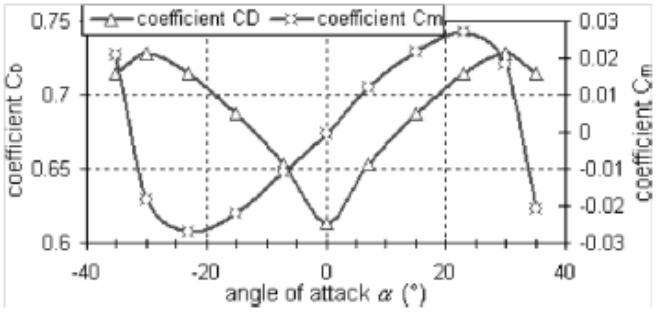

Figure 7.8 Parachute aerodynamic coefficients

The spatial angle of attack defined above denoted by α_{sp} and the other angles which are just its components, which are the angle of attack α and also the sideslip angle β are shown in figure 7.9. These angles help us in the determination of the moment coefficients in the different directions that is roll, pitch and yaw.

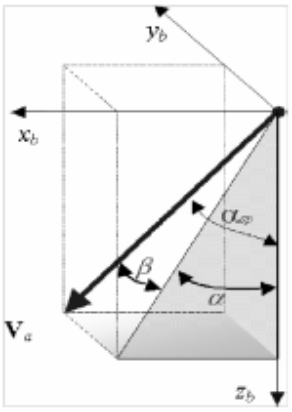

Figure 7.9 Spatial angle of attack determination

$$\alpha_{sp} = cos^{-1}\left(\frac{w_a}{\sqrt{u_a^2 + v_a^2 + w_a^2}}\right) \quad (7.24)$$

$$\alpha = tan^{-1}\left(\frac{u_a}{w_a}\right), \qquad \beta = tan^{-1}\left(\frac{v_a}{\sqrt{u_a^2 + w_a^2}}\right) \quad (7.25)$$

The wind vector Wu used in the Simulink model is given in the following way as:

$$V_a = V_R - {}^{u}_{b}R^{T} W_u \quad (7.26)$$

Here, R^T is the rotation matrix from the frame b to u.

Thus from the above it can be concluded that the force vector F_{Canopy} can be calculated as given below which only depends upon the spatial angle of attack as well on the

dynamic pressure. This force can be calculated on each axis of the parachute and then incorporated into the Simulink model.

$$F_{Canopy} = C_{Drag}(a_{sp})qS_0(V_a/\|V_a\|) \quad (7.27)$$

Where $q = 0.5\rho\|V_a\|^2$ is dynamic pressure; and $S_0 = \pi {R_0}^2$ the area of the canopy.

From reference [14] and [15] it can be assumed that the roll and the pitching moment values are the same for this parachute system that is,

$$C_{roll} = C_m(\beta), C_{pitch} = C_m(\alpha).$$

From the above the vector of the calculated moment about the three coordinate axes can be represented as below:

$$M_{canopy} = 2qS_0R_0 \begin{bmatrix} C_{roll} \\ C_{pitch} \\ C_n \end{bmatrix} \quad (7.28)$$

In equation (7.28) C_n is considered to be zero as it is the yaw moment representation here which turns out to be zero for this symmetrical parachute system.

Thus from the above mathematical equations formulated the six degree-of-freedom model was constructed using the SIMULINK software and the results are discussed as in the following part of the report.

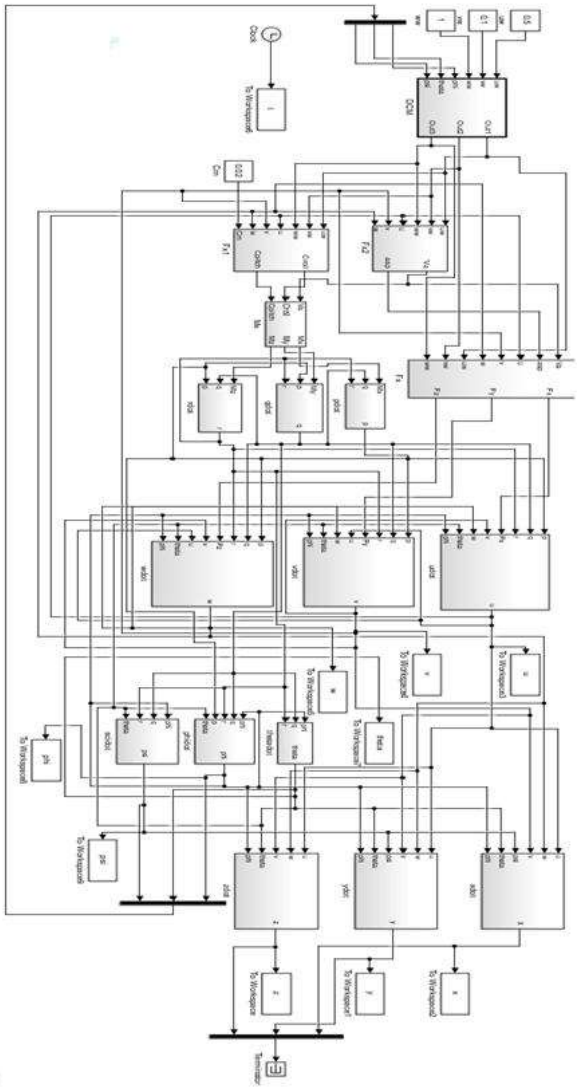

Figure 7.10 Simulink Model of Six-degree-of-freedom mode

VIII. AUTONOMOUS RECOVERY SYSTEM

Here in this chapter we are designing an autonomous recovery system for the SLYBIRD. The problem for any UAV arises when the battery potential falls below a threshold and the UAV cannot land before it falls so a suitable recovery system is needed which keeps on checking the battery level and switches off the motor and other equipments which drain the battery and opens the parachute for safe landing.

The recovery system designed here is based on the Arduino Nano. The microcontroller also uses the accelerometer and the GPS module coupled with it on a breadboard. The GPS module classifies the GPS coordinates, the accelerometer mounted is used so as to keep a check over the forces produced in the flight system and the main battery voltage is also being checked so that when the battery diminishes because of any reason during the flight of the

Slybird we can have the privilege to open the parachute system. The system designed here has been programmed in a manner that if it senses any problem as described below it will automatically instruct the servo motor to open the door of the spring loaded box of the parachute and lets the parachute to get out and hold the Slybird and help in landing it down safely. The problems discussed above are given below

- When the Slybird gets away from the sight of the operator the parachute system will automatically open and help in landing it down safely.
- When any type or freefall is being detected for 1 to 2 meters may be due to any reason and the operator loses control the parachute system will open.
- Also it will be operator controlled that is when it will come down in a normal manner to the prescribed landing height the system can be opened.

The Recovery system is very much required for the unmanned systems because the control over them is done by a remote operator and due to any circumstance if the connection is lost or the drone gets out of sight or any other problem occurs then atleast we can have it land on the ground safely without any disintegration of its parts. Further the design and other considerations are explained.

8.1 Parts of the Recovery system

The recovery system should be controlled independently of the UAVs flight controller, to ensure proper operation of the recovery system when the main battery has depleted. Thus for this condition a separate Arduino Nano microcontroller is used which is powered separately by a 7.4V Li-Po battery.

This microcontroller provides 14 Digital Input/output pins, 8 Analog pins, regulated 5V power source with a 16MHZ clock and 2Kb of SRAM. With this unit, all decision making process are completed. Each hardware component is connected to the microcontroller with the digital or analog pins.

8.1.1 Accelerometer

The accelerometer is connected to the microcontroller with the analog input pins. With the help of this the acceleration components in x, y and z direction are read according to voltage values generated. Since this module does not requires much current, analog output pins were sufficient to power the accelerometer.

A 3-axis accelerometer attached to the system constantly monitors the forces exerted on the UAV. The main reason of this to be used is to monitor the UAV for detecting free fall. The accelerometer here is used to monitor the force acting on UAV continuously so as to get a check when UAV falls due to unnecessary forces. In the case when the operator loses control over the UAV, where many UAVs cannot recover from free fall accelerations, the recovery system deploys the parachute and cuts power to the main control with a relay. The accelerometer detects free fall when the UAV experiences zero acceleration in x, y and z directions.

8.1.2 GPS

The GPS unit constantly checks position information (latitude, longitude, altitude and time) in National Marine Electronics Association (NMEA) (ASCII) format. The GPS module communicates with a RS232 serial connection to the Arduino Nano.

The operator has a complete view of the aircraft while in flight, If the UAV exceeds the predetermined range from its takeoff point, the recovery system will take over and cut power from the main system. Once the power is cut, the recovery system will deploy the parachute and land safely.

8.1.3 Voltage Sensor

The voltage sensor is connected to an analog pin on the microcontroller. The voltage sensor unit acts as a 4:1 voltage divider circuit, providing a voltage range within the limits of the analog-to-digital conversion circuitry on the Arduino's analog input pins.

The voltage sensor pulls a value continuously from the main battery source. Brushless DC motors often used on UAVs are voltage dependent that is the voltage of the power source primarily determines that the motors are able to be kept running. Lithium Polymer battery is used as these batteries have steady voltage until the battery reaches the end of charge. If the voltage of the main battery is inadequate, the system cut off power to the UAV via relay, and deploys the parachute for safe landing.

8.1.4 Servo Motor

The Servo motor is utilised to deploy the parachute which is contained in a spring loaded container. The servo motor is controlled via a Pulse Width Modulation (PWM) signal from the microcontroller's digital pins. The servo used, opens the spring loaded box and the chute deploys, this

happens due to the input from Arduino which processes any problem.

8.1.5 Relay Module 5 volts

The relay module is activated by a 5Vdigital signal from the microcontroller and cuts the power to the UAV's motors when activated. The relay used here was 'Active High', providing a 5Vsignal to the module which activates the internal switch.

8.1.6 Parachute

The parachute is being deployed from the spring loaded box using a servo motor at the door of the box. The parachute fabric is launched outward because of the spring force of the compressed spring placed in the box. The box can be 3D printed keeping in mind the size constraints as provided by the manufacturer of the UAV. For simplicity it can be constructed of a PVC tube, large spring, base plate and a servo motor holder.

The Figure below represents the schematic design of the recovery system.

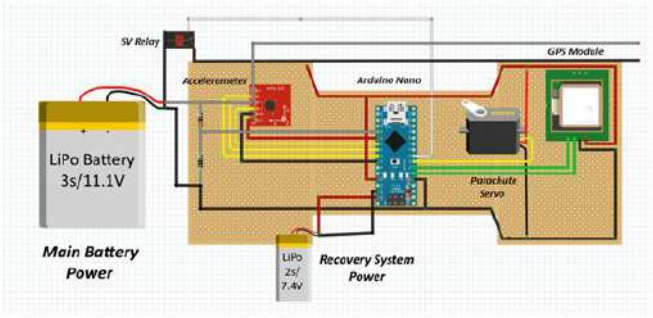

Figure 8.1 Design schematic of recovery system

8.2 Program Flowchart

The program continuously monitors three conditions to determine if UAV failure has occurred:

- Depletion of main battery voltage below a certain level.
- Free fall of UAV.
- UAV going beyond the line of sight from the operator according to GPS.

When the different values are being monitored, specific calibration is needed for proper use. The accelerometer values need to be set to detect free fall. The voltage sensor must also be calibrated to proper cut-off voltage of motors. The GPS should work efficiently and obtain the current position from satellites and compare the expected values stored in the microcontroller. The Flowchart of the process is given as below:

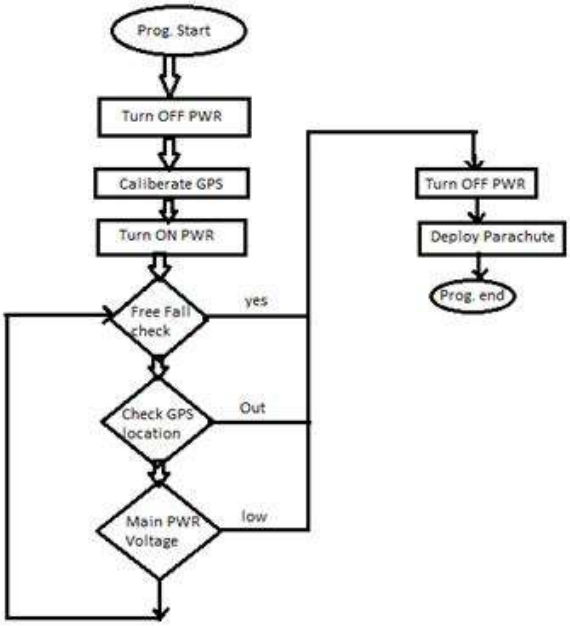

Figure 8.2 Flowchart of the recovery system program

The above described recovery system can be utilised to make the parachute deployment autonomous and thus the requirement of the project is completed. Further we go to the results generated by the six degree-of-freedom model.

IX. RESULTS AND DISCUSSIONS

The following results are generated from the Simulink model explained in chapter 7. The trajectory graph is as shown in the figure 9.1, is plotted in 3D which shows the wavy nature of the parachute falling to the ground with the UAV.

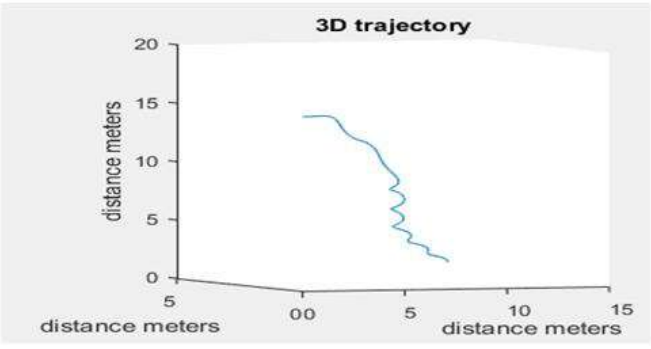

Figure 9.1 3D trajectory of the parachute with UAV

The vertical velocity graph is as shown in figure 9.2, where the velocity at the start is zero and it reaches to 3 m/sec also in the meantime because of the sudden opening of the parachute it fluctuates and as the wind is trying to pass through the parachute from bottom the velocity reduces also and it appears as if the chute is going upwards, but in the end after the required time of 10 seconds the velocity again reduces till 1m/sec or approximately zero and thus explains that the parachute with the payload lands very safely with very low vertical velocity and thus the Slybird remains safe, as the safe landing velocity calculated in the previous chapters was nearly equal to 4m/sec. But here it is being reduced to 1m/sec, thus the parachute designed is in compliance with the desired problem.

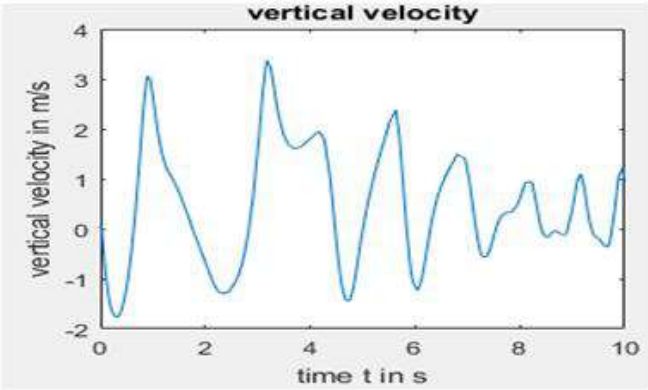

Figure 9.2 Vertical velocity of the falling parachute

The altitude at which the parachute is opening is assumed to be 15 meters, and thus the altitude reduction graph is shown in figure 9.3 which reduces to zero in approximately 10 seconds. The Model generated also generates the different angle graphs and the forces which act in particular x, y and z directions.

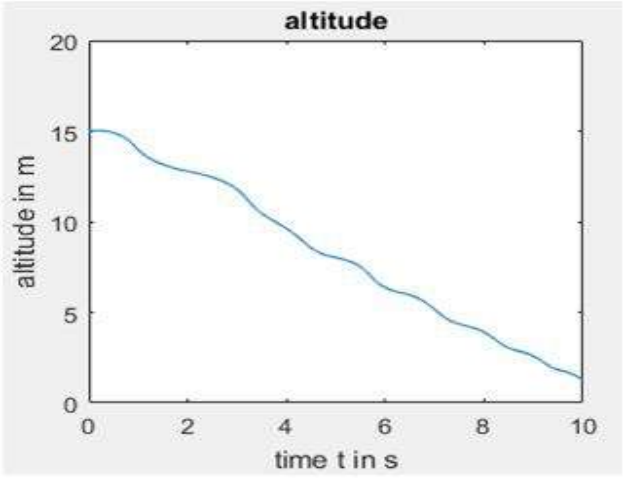

Figure 9.3 Altitude reductions with respect to time

By changing the various parameters like the suspension line lengths and the canopy area the values recorded change and various different graphs can be generated.

X. CONCLUSION

The project represents the results of the development of six degree-of-freedom model of the circular parachute canopy. Key contributions of the project include the following:

- Development of a six degree-of-freedom model for a circular parachute with elaborated study over the different aspects of opening forces and other parameters.
- Providing an autonomous mechanism so as to build a recovery system for UAVs. The codes over Arduino are simple and so not provided here.

The model developed gives the permissible results, however further improvement is possible. It includes involving more optimized parameters into the model development equations. The parachute can also be controlled using actuators which control the riser or suspension line lengths and hence control the manoeuvrability of the parachute.

As the parachute was opening at very low altitude so the concept of added mass is not considered. Due to less height the control of the parachute was also not possible. Further study may involve theses parameters so as to get a controlled autonomous parachute.

XI. ACKNOWLEDGEMENT

At first I thank Almighty for guiding me in every step on my way to the completion of this project.

I would like to thank Dr. Anand Swaroop Verma (Associate Professor & Head) , in Department of Mechanical Engineering for allowing me to work for the project in the Institution and to give me the desired division to showcase my skills. I am thankful to and fortunate enough to get constant encouragement, support and guidance from my guide Dr. Brajesh Vashney Sir, Director of Kanpur Institute of Technology ,who helped me in successfully completing the project work.

My sincere thank to Ms. Smita Dwivedi , Assistant Professor Mechanical Department, and all the faculty

members of Mechanical Engineering Department for their support and help they have provided..

I heartily thank my internal project guide, Dr. Anand Swaroop Verma aa, Assistant Professor (Mechanical Department), Kanpur Institute Of Technology, Rooma Kanpur, for his guidance and suggestions in compilation of the project work. In the end I would like to bestow my regards to my family and friends for their untiring love and enduring support which was inevitable for the success of all my ventures.

REFERENCES

[1] Terms and Symbols for Flight Dynamics - Part 1: Aircraft Motion Relative to the Air. International Standard *1151. International Organisation for Standardization, Second Edition-1975*
[2] Ludtke, W.P. Effects of Canopy Geometry on a Cross parachute in the Fully Open and Reefed Conditions. For a W/L Ratio of 0.264. U.S. *Naval* Ordnance Laboratory, NOLTR 71-111, August 1971
[3] *Performance of and Design Criteria for Deployable Aerodynamic Decelerators. U.S.* Air Force Flight Dynamics Laboratory, Ohio Technical Report ASD TR.61.579 December 1963
[4] Ludtke, W.P Alternate Altitude testing of solid cloth parachute systems, NSWC TR 85-24
[5] Ludtke, W. P., Observations on Parachute Scale Factors for Modelling Parachute Deployment and Steady State Performance, NSWC/WOL TR 78-189
[6] Knacke T.W and Hegele A.M Model Parachutes : Comparison test of various types. US Air Force/ Aeronautical Systems Division Report MCREXE-672-12D, January 1949
[7] Observations on the Inflation Time and Inflation Distance of parachutes, William P Ludtke.
[8] Tory,C and Ayres, R.,"Computer Model of a Fully Deployed Parachute," Journal of Aircraft , Vol 14, No.7,1977, pp 675-679.
[9] Tuma, J.J, Engineering Mathematics Handbook, McGraw hill, New York, 1987.
[10] Favorin,M.V.,Momenti Inerzii Tel. Spravochnik(Moments of Inertia Of Bodies, Reference Book), Mashinostroenie, Moscow,1977(in Russian).
[11] Knacke, T.W, Parachute Recovery System Design Manual, Para Publishing, Santa Barbara,CA 1992.
[12] Moseev, Yu," Fluid-Structure interaction Simulation of the U.S Army G-12 parachute,"
[13] White ,F.M.,and Wolf,D.F., " A Theory of Three dimensional Parachute Dynamic Stability," Journal of Aircraft, Vol.5, No,1 1968,pp. 86-92.
[14] Etkin, B., Dynamics of Flight,Wiley,New York , 1959
[15] Schmidt, L., Introduction to Aircraft Flight Dynamics, AIAA,Reston,VA 1998.
[16] Vladimir N.Dobokhodov, Oleg A Yakimenko.,'Six degree of freedom model of a controlled circular parachute'.
[17] Yavus, T., and Cockrell, D. J., "Experimental determination of Parachute Apparent Mass and its significance in Predicting Dynamic Stability," Proceedings of 7th AIAA Aerodynamic Decelerator and Balloon Technology Conference, New York 1981.
[18] Yavuz,T., "Determining and Accounting For a Parachute Virtual Mass," Journal of Aircraft, Vol 26, No.5, 1989. Pp 432-437.
[19] Doherr, K-F., and Saliaris, C., "On the influence of Stochastic and Acceleration Dependent Aerodynamic Forces on The Dynamic Stability of Parachutes," Proceedings of 7th AIAA Aerodynamic Decelerator and Balloon Technology Conference, New York 1981.
[20] Cockrell., D.J., and Doherr, K.-F., "Preliminary Consideration of Parameter Identification Analysis From Parachute Aerodynamic Flight-Test Data," Proceedings of 7th AIAA Aerodynamic Decelerator and Balloon Technology Conference, New York 1981.
[21] Wikipedia.
[22] National Aerospace Laboratory, website for knowledge over Slybird

Appendix

The Matlab Code used with the Simulink model is given as below:

```
Clear;
%ADS components masses
%e =0.8 ratio of minor to major axis (canopy shape ratio)between 0.5-1
g = -9.81;
gama =0.2617;% 15 degree cone half agle [gamma = asin(((Rp-a)/sqrt2)*(1/(Lsl+Lpma)))]
L =2;%length in meters
a =0.15 ; %meters side of payload
C = cos(gama);
S = sin(gama);


m1 = 0.300; % kg mass of canopy
m2 = 0.200; % kg mass of susp line
m3 = 0.0; % kg mass of actuator PMA
m4 = 4.0; % kg mass of payload

m = m1+m2+m3+m4; % total mass
```

```
% ADS components dimensions

R0 = 2;          % Radius of UNinflated canopy
Rp = 2*R0/3;       % Radius of inflated canopy

% Moment of Inertia of canopy
Ixc=0.246*m1*Rp^2*2.22;
Izc=0.66*m1*Rp^2*0.9680;

% Moment of Inertia of suspension line
Ixs= 0.5*m2*(L^2*(1+C^2)/12+(Rp-(L*S/2)));
Izs= m2*(L^2*S^2/12 + (Rp - (L*S/2)));

% Moment of Inertia of payload
Ixp=m3*a^2/6;
Izp= Ixp;

% Transferring individual inertia components to the origin of B using
% parallel axis theorem
Icc = Ixc+ m1*(-Rp/2)*0.83;
Iss = Ixs+ m2*(L*C*0.5);
Ipp = Ixp + m4*(a/2);
% Total moment of Inertia
Ix = Icc+Iss+Ipp;
Iy = Ix;
Iz = Izc + Izs + Izp;

CD = -0.75; %0.6 to 0.8
S0 = pi*R0^2;
rho =1.225;

%Cm =0.01;
%ASSUMING VALUES

Cyaw =0;

sim('parachute.slx');

%phi = roll angle
%theta = pitch angle
%psi = yaw angle

V = sqrt(u.^2+v.^2+w.^2);
close all;
figure(2)
subplot(2,3,1);
plot(t,V);
axis([0 12 0 10]);
xlabel('time t in s');
ylabel('absolute velocity metres');
title('Velocity');
subplot(2,3,2);
plot(x,y);
xlabel('X in m')
ylabel('Y in m')
title('Top view of trajectory')
axis([-2 100 -2 100])
subplot(2,3,3);
plot3(x,y,z);
zlim([0 20]);
xlim([0 10]);
ylim([0,15]);
xlabel('distance meters');
ylabel('distance meters');
zlabel('distance meters');
title('3D trajectory');
subplot(2,3,4);
plot(x,z);
xlabel('x in meters');
ylabel('z height in meters');
title('Front view of trajectory');
subplot(2,3,5);
plot(t, w);
xlabel('time t in s');
ylabel('vertical velocity in m/s');
title('vertical velocity');
subplot(2,3,6);
plot(t,z);
xlabel('time t in s');
ylabel('altitude in m');
title('altitude');

%Graphs for roll pitch and yaw angles
figure(1)
subplot(1,3,1);
plot(t,phi);
xlim([0 10]);
xlabel('time t in s');
ylabel('Roll angle');
title('Roll angle graph');
subplot(1,3,2);
plot(t,theta);
xlabel('time t in seconds');
xlim([0 10]);
ylabel('pitch')
title('Pitch angle ');
subplot(1,3,3);
plot(t,psi);
xlabel('time t in seconds');
ylabel('yaw');
xlim([0 10]);
title('Yaw angle');
```